



Contents lists available at ScienceDirect

Engineering

journal homepage: www.elsevier.com/locate/eng

Research

Next Ten Years: Create a Better Future—Review

Mixing Intensification for Advanced Materials Manufacturing

Chao Yang^{a,c,#}, Guang-Wen Chu^{b,d,#}, Xin Feng^{a,c}, Yan-Bin Li^{b,d}, Jie Chen^{a,c}, Dan Wang^{b,d}, Xiaoxia Duan^{a,c}, Jian-Feng Chen^{b,d,*}^a State Key Laboratory of Biochemical Engineering & Key Laboratory of Green Process and Engineering, Institute of Process Engineering, Chinese Academy of Sciences, Beijing 100190, China^b State Key Laboratory of Organic-Inorganic Composites, Beijing University of Chemical Technology, Beijing 100029, China^c School of Chemical Engineering, University of Chinese Academy of Sciences, Beijing 100049, China^d Research Center of the Ministry of Education for High Gravity Engineering and Technology, Beijing University of Chemical Technology, Beijing 100029, China

ARTICLE INFO

Article history:

Received 26 October 2024

Revised 11 December 2024

Accepted 21 December 2024

Available online xxx

Keywords:

Mixing intensification

Chemical reaction

Advanced materials

High-end manufacturing

ABSTRACT

The mixing process plays a pivotal role in the design, optimization, and scale-up of chemical reactors. For most chemical reactions, achieving uniform and rapid contact between reactants at the molecular level is crucial. Mixing intensification encompasses innovative methods and tools that address the limitations of inadequate mixing within reactors, enabling efficient reaction scaling and boosting the productivity of industrial processes. This review provides a concise introduction to the fundamentals of multiphase mixing, followed by case studies highlighting the application of mixing intensification in the production of energy-storage materials, advanced optical materials, and nanopesticides. These examples illustrate the significance of theoretical analysis in informing and advancing engineering practices within the chemical industry. We also explore the challenges and opportunities in this field, offering insights based on our current understanding.

© 2025 THE AUTHORS. Published by Elsevier LTD on behalf of Chinese Academy of Engineering and Higher Education Press Limited Company. This is an open access article under the CC BY-NC-ND license (<http://creativecommons.org/licenses/by-nc-nd/4.0/>).

1. Introduction

Chemical reactors, in which raw materials are transformed into final products, are central to all chemical process industries. The efficiency of chemical reactions is inherently dependent on the physical mixing process, as reactants must come into molecular-scale contact with each other to react. Consequently, mixing directly influences the production capacity of a reactor. In complex competitive reactions, the local concentrations of reactants—which are controlled by mixing—significantly affect the selectivity of the desired products and, ultimately, the overall production efficiency. Therefore, the mixing process holds substantial academic significance and practical engineering value in the design, optimization, and scale-up of reactors [1].

Although no explicit quantitative relationships have been established between mixing and reaction efficiency, their correlation is often qualitatively positive. To systematically address such relationships, the mixing process is commonly categorized into

the two scales of macromixing and micromixing, based on differences in length scale [2]. *Macromixing* occurs at the reactor scale and involves the dispersion of materials over large distances through bulk convection and eddy diffusion. This process establishes the local concentration conditions that facilitate micromixing. *Micromixing*, on the other hand, operates near the molecular scale and encompasses phenomena such as vortex engulfment, the deformation of micro-clumps at the Kolmogorov scale, and molecular diffusion. Macromixing enhances micromixing by increasing the interfacial area for molecular diffusion between bulk regions with differing properties, thereby shortening diffusion distances. Some studies further classify eddy diffusion as an intermediate scale, termed “mesomixing,” thus distinguishing it from macromixing [3]. While this perspective is valid, the term “mesomixing” is less commonly used in most works.

2. Multiphase mixing

2.1. Experimental measurement

In the study of multiphase flow systems within reactors, accurate local flow field measurements are essential for understanding

* Corresponding author.

E-mail address: chenjf@mail.buct.edu.cn (J.-F. Chen).

These authors contributed equally to this work.

<https://doi.org/10.1016/j.eng.2024.12.019>

2095-8099/© 2025 THE AUTHORS. Published by Elsevier LTD on behalf of Chinese Academy of Engineering and Higher Education Press Limited Company.

This is an open access article under the CC BY-NC-ND license (<http://creativecommons.org/licenses/by-nc-nd/4.0/>).

the complex interactions that occur among different phases. These measurements form the foundation for optimizing reactor design and operation by providing essential information on flow patterns, phase distribution, and dynamic interactions. Current measurement techniques are categorized by their level of invasiveness and the timeliness of data acquisition, ranging from invasive to non-invasive methods and from real-time to non-real-time data. These techniques leverage approaches and principles such as visual and microscopic observations, laser technology, image processing, spectroscopy, acoustics, optical interference, and electrical characteristics [4]. Selecting the appropriate technique requires maintaining a careful balance between minimizing system disturbance and maximizing data accuracy.

Among these techniques, telecentric photography stands out for its exceptional ability to deliver detailed, *in situ* visualizations of multiphase flow phenomena, enabling researchers to capture high-resolution images that clearly depict phase boundaries and interactions. Similarly, high-speed cameras have transformed the study of fast transient phenomena, allowing researchers to observe rapid processes that govern phase interactions and mixing efficiency. For example, Chen et al. [5] pioneered the use of high-speed stroboscopic microscopic photography to visualize fluid elements during mesoscopic and microscopic mixing processes, which has yielded valuable insights into micromixing behavior. Additionally, the high-speed telecentric imaging of vortex engulfment has provided quantifiable insights into micromixing processes, offering a deeper understanding of how to enhance chemical reaction rates and overall reactor performance as shown in Fig. 1 [6].

The chemical probe method is a convenient and intuitive approach to characterize the mixing performance of reactors. Its core principle relies on reaction systems that are highly sensitive to mixing, where the intrinsic reaction rate significantly exceeds the mixing rate. In such systems, the macroscopic reaction rate is governed by mixing, enabling the quantitative evaluation of mixing effects [7]. Compared with physical measurement methods and computational fluid dynamics (CFD), the chemical probe method provides direct, quantitative insights into mixing efficiency across different scales and operating conditions without requiring complex equipment or extensive computations. Moreover, it is versatile and applicable across various reactor structures [8].

In liquid–liquid heterogeneous systems, where the mixing time is often predominantly influenced by the interfacial mass transfer resistance, chemical probe systems are categorized into single, parallel, and continuous competitive reaction systems. Common single reaction systems include acid–base neutralization, such as the reaction of sodium hydroxide with acetic acid, and alkaline hydrolysis reactions, such as the saponification of ethyl benzoate with sodium hydroxide [9]. Parallel competitive systems, like the neutralization of benzoic acid combined with the alkaline hydrolysis of ethyl chloroacetate, characterize liquid–liquid heterogeneous mixing through byproduct selectivity. These systems are stable, sensitive, and effective for assessing mixing performance, although the byproduct selectivity depends on both mixing performance and reactant properties, such as diffusion and distribution coefficients [10]. For continuous competitive systems, Zhang et al. [11] developed an alkaline hydrolysis probe for acetylsalicylic acid, which effectively characterizes mixing performance under varying conditions, including different mixing intensities, oil–water ratios, and co-solvent concentrations.

As multiphase flow measurement technologies advance, their integration into industrial applications is increasingly prioritized. The transition from laboratory tools to robust, scalable industrial solutions necessitates technologies that are precise and efficient. Coupling advanced measurement techniques with computational

models, such as CFD, enhances predictive accuracy and reactor design optimization. This integration enables detailed simulations of observed phenomena, the validation of models, and the exploration of operational scenarios, thereby reducing experimental costs and risks.

The integration of artificial intelligence (AI) has further revolutionized data analysis in this field. AI enables dynamic process adjustments and improved reactor performance optimization, particularly through the image-based analysis of multiphase flows. Convolutional neural networks (CNNs) have demonstrated exceptional performance in tasks such as multiphase flow image analysis, offering resilience against variations in lighting and noise [12–14]. However, their dependence on large, labeled datasets and substantial computational resources limits their broader application.

To address these challenges, foundational models represent a significant advancement. These pretrained neural networks, built on extensive and diverse datasets, offer superior generalization capabilities. For example, the bubSAM, derived from the Segment Anything Model (SAM), excels in bubble segmentation and shape reconstruction under zero-shot conditions in bubbly flow images [15]. As shown in Fig. 2 [15], bubSAM performs well under varying aeration conditions, reducing the data dependency typical of CNNs and minimizing retraining requirements for new applications. Such innovations increase the feasibility of deploying these models in dynamic industrial environments, thus meeting the evolving demands of reactor optimization.

The integration of AI with traditional measurement techniques represents a significant advancement in the analysis of multiphase flow systems. By leveraging the predictive capabilities of neural networks, researchers can dynamically adjust processes and optimize reactor performance with unprecedented precision. This fusion improves measurement accuracy and enhances the scalability and practicality of deploying these advanced technologies in real-time, high-stakes industrial environments. The future evolution of these systems will be based on the development of less invasive, more automated measurement solutions, using machine learning to provide real-time, high-resolution data.

2.2. Macromixing

2.2.1. Experimental

Macromixing has been extensively studied over a long period of time, and related research methods and findings are both well-established. The quality and rate of macromixing can be assessed using quantitative indicators; of these, the most commonly used is the mixing time, which refers to the time required for the material within the reactor to reach a certain degree of macroscopic uniformity [16]. For continuous flow reactors, the residence time distribution (RTD) is also employed to reveal the mixing characteristics of the flow [17].

Primary research methods for mixing include tracer experiments and CFD numerical simulations, with several comprehensive reviews of the former being available [18,19]. Factors such as the choice of tracer, feed position and approach, detection position and probe size, chemical processes involved, and data-processing techniques for tracer signals all influence the accuracy and precision of mixing time measurements. However, tracer experiments are ideally conducted on physical processes without chemical reactions to eliminate interference from micromixing.

2.2.2. Simulations

When designing and optimizing industrial reactors, it is often insufficient to solely rely on experimental methods. Consequently, various mathematical models have been developed to calculate mixing time. The mechanisms of macromixing in single-phase systems are thoroughly understood, which has led to the creation of

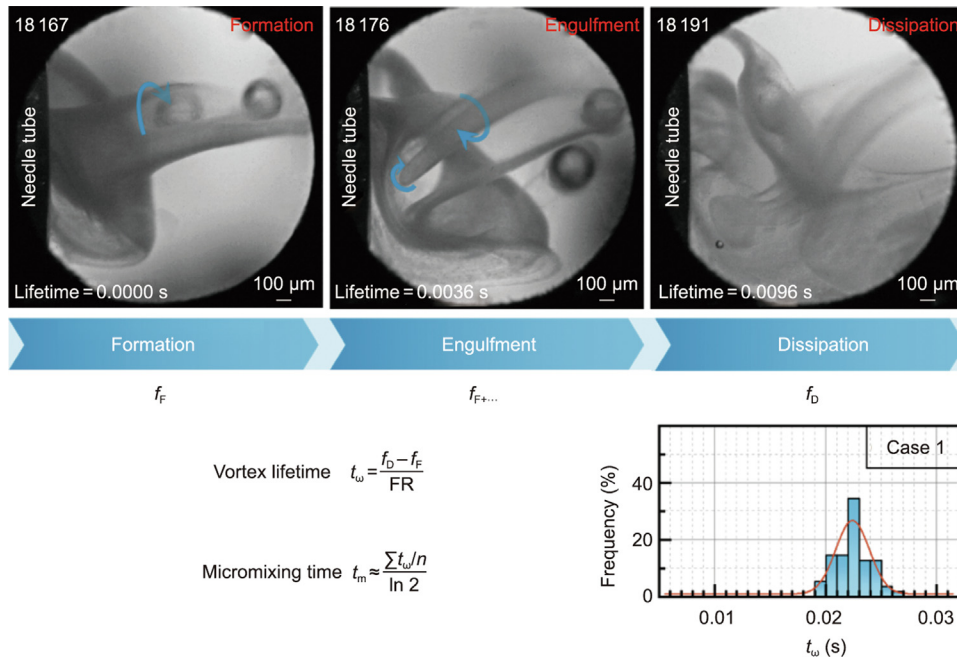


Fig. 1. Telecentric photography reveals engulfment vortex behavior, lifetime, and micromixing time. f_F , $f_{F+...}$, and f_D are the key frames for the formation, engulfment, and dissipation of vortices, respectively; t_w and t_m are the vortex lifetime and micromixing time, respectively; n is the number of vortices; and FR is frame rate. Reproduced from Ref. [6] with permission.

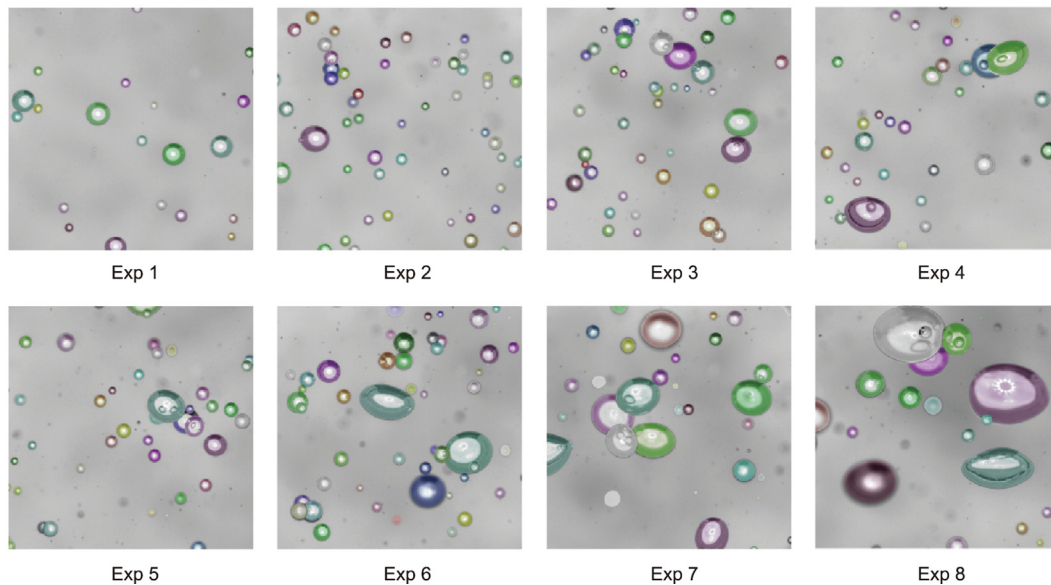


Fig. 2. Examples of segmentation results obtained from bubSAM under different aeration rates ($L \cdot \text{min}^{-1}$): 0.09 for experiment (Exp) 1, 0.18 for Exp 2, 0.27 for Exp 3, 0.36 for Exp 4, 0.45 for Exp 5, 0.54 for Exp 6, 0.63 for Exp 7, and 0.72 for Exp 8. Reproduced from Ref. [15] with permission.

several empirical models, circulation models [20,21], diffusion models [22–24], compartmental models [25,26], and CFD models. The first four types of models rely on experimental data correlations or approximate calculations, which lack general applicability and often fail to accurately represent actual flow conditions within reactors.

CFD methods offer a powerful tool for simulating macromixing in reactors and obtaining global mixing parameters [27]. The current trend in theoretical studies on macromixing is to develop mechanistic mixing models with suitable numerical solutions. The convective diffusion equation of a tracer scalar describes how the tracer progressively achieves uniform mixing within a

reactor. As illustrated in Fig. 3 [28], by coupling the pulse input method with the stabilized flow field in a spinning-disk reactor to simulate the RTD, real-time variation in the tracer concentration and the homogenization process can be tracked within the complex reactor structure. This highlights one of the key advantages of numerical simulation over conventional experimental measurements. By quantifying the average residence time and dimensionless variance, CFD simulations can effectively assist in reactor design and optimization.

CFD simulation offers significant advantages in macromixing due to its precise control over tracer injection rates [29]. For equipment with short residence times, such as spinning-disk reactors

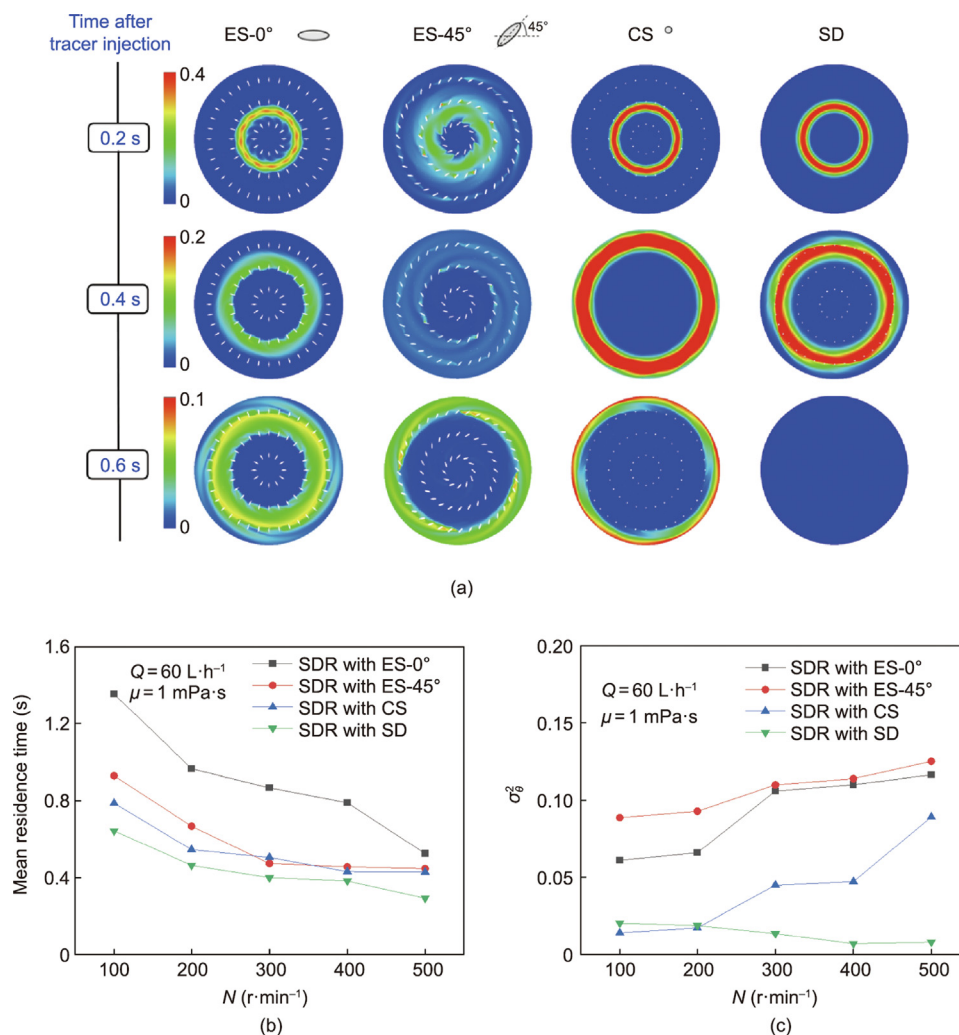


Fig. 3. Macromixing simulation of RTD in a spinning-disk reactor with different disk configurations. (a) Temporal tracer molar fraction distribution; (b) mean residence time; (c) dimensionless variance. ES: elliptic-cylindrical spoilers; CS: cylindrical spoilers; SD: smooth disk; SDR: spinning-disk reactor; N : rotational speed; Q : liquid flow rate; μ : liquid dynamic viscosity; σ^2 : dimensionless variance. Reproduced from Ref. [28] with permission.

and rotating packed-bed (RPB) reactors, the development of CFD simulation methods is particularly crucial. Given the significant advances in computational capabilities, the accuracy of numerical simulations now rivals that achieved by empirical correlations and simpler mixing models, broadening their range of application. It is important to note that accurate simulation of fluid flow serves as the foundation for further macromixing simulations.

2.3. Micromixing

2.3.1. Experimental

Micromixing, which corresponds to mixing at smaller scales, refers to the homogenization process of components from the Kolmogorov scale ($\sim 10^{-4}$ m) to the molecular scale ($\sim 10^{-9}$ m). Since the inception of chemical engineering, micromixing has been a focal point due to its significant impact on reaction processes, especially in fast competitive reactions. The molecular scale is too small to be observed with physical methods such as optical or microscopic instruments; however, at scales above the micron level, optical measurements can capture some local flow field information, thereby linking fluid dynamic heterogeneity with micromixing environments [6].

Due to the lack of sufficiently high spatial resolution to directly depict micromixing, micromixing time is commonly used as an

indirect indicator of micromixing efficiency. The micromixing time is the characteristic time required for components to achieve molecular homogenization. When the micromixing time exceeds the characteristic time of the chemical reactions involved, part of the local concentration driving force is spent on promoting micromixing, rather than being fully utilized for the chemical reaction. This results in a reaction rate lower than the predicted rate based on intrinsic kinetics. Additionally, in the case of competitive side reactions, byproducts may be formed.

To address this issue, several chemical reaction systems sensitive to mixing have been developed to assess micromixing efficiency based on characteristic reaction time. The local concentration controlled by micromixing plays a significant role in determining the product distribution of chemical reactions. Many reviews have been published on test reactions [7,8], which can be categorized into three types, as summarized in Table 1 [11,30–38]. These test reactions are based on how mixing influences reaction selectivity, with the segregation index (X_S) serving as a quantitative measure. The segregation index, which varies depending on the test reaction, can be used to assess the selectivity of side reactions. (For specific reaction principles, interested readers can refer to the references in Table 1.) The test reactions generally follow the principle that the reaction rate approaches the rate predicted by the intrinsic kinetics when micromixing is optimal,

Table 1
Three types of test reaction systems.

Type	Formula	Indicators	Typical examples	Refs.
Single reaction	$A + B \rightarrow R$	Reaction rate or conversion rate Grain size and morphology	Alkaline hydrolysis of nitromethane Precipitation of barium sulfate	[30] [31]
Parallel reaction	$A + B \rightarrow R$ $A + C \rightarrow S$	Reaction selectivity (X_S)	Acid–base neutralization and alkaline hydrolysis of ethyl chloroacetates Villermoux–Dushman test reaction	[32,33] [34]
Consecutive reaction	$A + B \rightarrow R$ $R + B \rightarrow S$	Reaction selectivity (X_S)	Acid–base neutralization and alkaline hydrolysis of diethyl oxalate Diazo coupling between 1-naphthol and diazotized sulfanilic acid Consecutive hydrolysis of acetylsalicylic acid	[35] [36,37] [11,38]

whereas poor micromixing leads to deviations. To quantify this principle, the segregation index is defined to evaluate the selectivity of side reactions in the test systems. When the characteristic reaction time is shorter than the micromixing time, the segregation index is primarily controlled by micromixing. The mathematical form of the segregation index may differ across test reactions, but it is generally normalized and ranges from 0 to 1. A value closer to 1 indicates poorer micromixing.

2.3.2. Modeling

Based on theoretical analyses of experimental results, several micromixing models have been proposed. Phenomenological models such as the coalescence–redispersion model [39], the multi-environments model [40], and the interaction by exchange with the mean (IEM) model [41] were the first to be introduced. These models rely on one or more empirical parameters to describe an intermediate state between perfect mixing and complete segregation, treating the reactor as a “black box.” Fournier et al. [42] proposed an incorporation model that uses micromixing time as a parameter in ordinary differential equations to describe a reaction process in which reactants are consumed within micro-clumps. Based on the Lagrangian method, this model tracks the reaction and volume expansion of a micro-clump injected into the reactor. The assumption that a micro-clump’s volume grows exponentially is physically realistic and has been successfully applied to the Villermoux–Dushman test reaction. When predicting the segregation index of test reactions using this model, careful consideration must be given to factors such as the correct handling of local concentration and ensuring material balance [43].

Nevertheless, empirical models lack a solid theoretical foundation in fluid mechanics and cannot quantitatively or qualitatively predict experimental results with high accuracy. The parameters in such models are generally obtained through curve fitting, which inherently limits their applicability. To address this limitation, mechanistic models have been developed that incorporate physical and chemical mechanisms alongside mathematical expressions that better reflect the micromixing process. Since micromixing operates through molecular diffusion at the microscale, the spatial domain size of the micromixing process must be considered. Without this, the concept of local concentration becomes meaningless. Nearly all mechanistic models describe the micromixing process from micro-clumps at the Kolmogorov scale downward, taking into account the enhancement of molecular diffusion by turbulence at the Kolmogorov scale, as illustrated in Fig. 4. Although models such as the engulfment model [44,45], the shrinking-slab model [46], and the cylindrical stretching vortex model [46] have been validated through optical experiments [6,47–49], previous reviews [2] have highlighted their theoretical shortcomings. Numerically solving these mechanistic models is challenging and often requires simplifications, which can limit their applicability. For example, the generalized application of the engulfment model is only valid for fluids with a Schmidt number (Sc) much smaller than 4000. Under these conditions, deformation of the engulfing vortex and molecular diffusion can be neglected. The model assumes isotropic

and homogeneous turbulent flow under high-Reynolds-number conditions; however, in reality, even at high Reynolds numbers, the flow can exhibit anisotropy.

The incorporation model is widely used due to its simplicity and its ability to directly estimate the micromixing time (t_m) [50–52]. Based on this model, Zhang et al. [11] developed an alkaline hydrolysis probe system for acetylsalicylic acid and, by combining it with Kolmogorov turbulence theory, established a formula for estimating the micromixing time in a standard stirred tank: $t_m = 13.956(\nu/\varepsilon)^{0.5}$ (ν is the kinematic viscosity ($N \cdot s \cdot m^{-2}$) and ε is the energy-dissipation rate ($W \cdot kg^{-1}$)). Using the same probe system, Zhang et al. [38] quantitatively characterized the heterogeneous liquid–liquid mixing efficiency in an RPB reactor under various operating conditions. By measuring the diameter of dispersed phase droplets in the RPB, they derived a relationship for predicting the average droplet diameter based on the Hinze–Kolmogorov theory:

$$d_{32} = 0.151(1 + 8.8\phi)(\sigma/\rho_c)^{3/5}\varepsilon^{-2/5} \quad (1)$$

where d_{32} is the Sauter mean diameter (m), ϕ is the volume fraction of dispersed phase, σ is interfacial tension ($N \cdot m^{-1}$), and ρ_c is the carrier-phase density ($kg \cdot m^{-3}$). From the dispersed phase size and mass transfer characteristics, they also developed a model to predict the partition factor of heterogeneous liquid–liquid mixing in the RPB, achieving an error of less than $\pm 20\%$.

Mixing, which includes both macromixing and micromixing, encompasses different mechanisms of the same process. While these can be roughly separated in space and time, they cannot be completely isolated. Therefore, accurate numerical simulations must treat them as an integrated whole. Significant progress has been made in combining CFD methods with micromixing models to describe fluid mixing at various scales. In reactors, micro-clumps move through space while interacting with their surroundings, mixing, and reacting [53]. Their movement paths and the energy-dissipation rates along these paths, which were previously difficult to determine experimentally, can now be more easily obtained using CFD methods [54]. A practical approach involves first conducting macroscale CFD simulations using Reynolds-averaged or large-eddy simulation methods and then calculating the mixing–diffusion reaction at the sub-grid scale, which requires a suitable micromixing model for CFD simulation. Thus, the critical and challenging task is to develop new micromixing models, establishing comprehensive mechanistic mathematical models and full spatiotemporal numerical simulations that incorporate all physical and chemical processes to accurately reflect the mixing process. Duan et al. [55] developed a coupled CFD-engulfment (CFD-E) model for multiphase micromixing based on Eulerian–Eulerian multiphase flow. They investigated the micromixing effects on parallel competing chemical reactions occurring in multiphase stirred tanks, using more physically relevant model parameters such as the mixed fraction and its variance. The predicted segregation index under various operating conditions showed reasonable agreement with the experimental data (Fig. 5) [55].

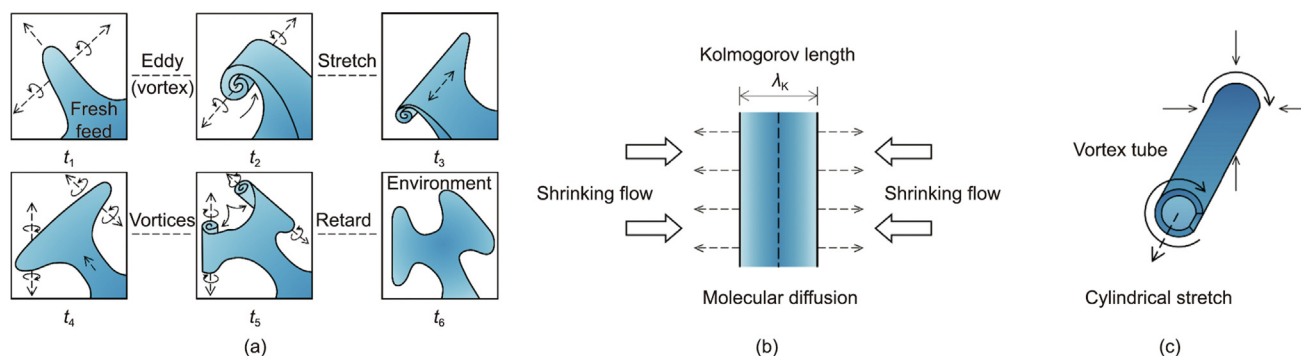


Fig. 4. Micromixing mechanism models based on the Kolmogorov scale. (a) Engulfment model; (b) shrinking-slab model; (c) cylindrical stretching vortex model. (a) Reproduced from Ref. [6] with permission.

Since the importance of micromixing in chemical reaction engineering was first recognized in the 1950s, research into the mechanisms of micromixing and the application of its models has been ongoing. As far as model application and solution convenience are concerned, it is hoped that a key time parameter—equivalent to the micromixing time—can be included to characterize the efficiency of micromixing. Although the incorporation model and the engulfment model describe different physical concepts of growing zones, both employ similar numerical methods and solving processes have been widely used for predicting the segregation index. However, reports on mechanistic models of micromixing in multiphase reaction systems remain scarce. The presence of an inert phase can influence the dispersion of fluid clusters and alter the boundary conditions of cluster microelements in micromixing models. While experimental research on multiphase micromixing continues to progress, it largely focuses on test reactions with limited extension to heterogeneous systems. The real challenge lies in expanding these studies to the multiphase systems common in the process industry, in which reactants form different phases. Interphase mass transfer mechanisms and the influence of the dispersed phase on the local flow field of the continuous phase must also be considered.

Moreover, it should be noted that most studies on macromixing and micromixing focus on low-viscosity liquid systems, with fewer investigations having been carried out on polymer systems. Although some theories and methodologies developed for low-viscosity liquid systems—such as RTD and CFD simulations—can be applied to polymer systems [56–59], those related to micromixing are not directly applicable. This is because, in polymer systems, multiscale diffusion and flow-induced dynamics play critical roles. Unlike small-molecule systems, polymer mixing is affected by the constrained diffusion of entangled chains and the faster mobility of chain ends. The rate of polymer chain diffusion is highly dependent on polymer chain orientation, which is influenced in turn by the type and strength of the flow. In shear-dominated flows, chains align along the flow direction, reducing entanglements and increasing diffusion rates. Conversely, in extensional flows or weaker flow fields, chains exhibit random or isotropic orientations, slowing diffusion. At interfaces, the interdiffusion of chain ends—being more mobile and less entangled—drives efficient mixing and stabilization, which are critical for applications such as polymer blending [60–63]. These flow-dependent and scale-dependent diffusion behaviors present challenges for reactor design [64,65]. Effective macromixing strategies must address the slower diffusion of bulk polymer chains, while micromixing approaches should capitalize on the increased mobility of chain ends, particularly at interfaces [66,67]. By tailoring flow fields to optimize chain orientation and interdiffusion, mixing efficiency and reaction uniformity can be significantly improved.

3. Applications

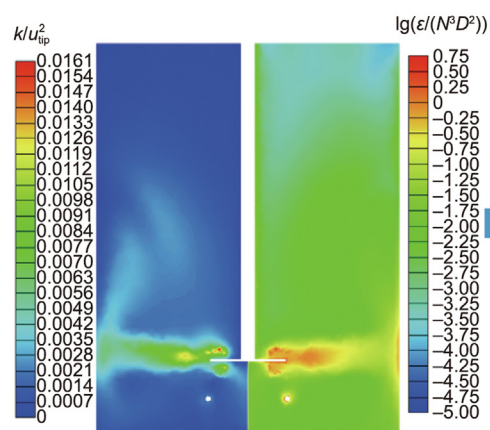
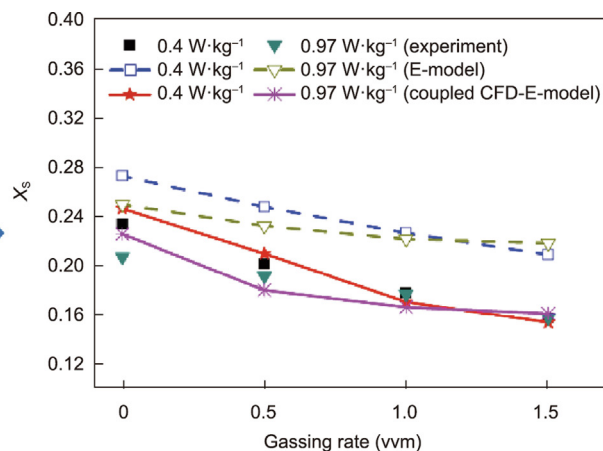
It has been demonstrated that mixing intensification can enhance reaction efficiency, increase conversion rates, and reduce raw material and energy consumption [68–71]. The theory of mixing intensification has seen numerous successful applications in chemical industrial processes, particularly in the petrochemical industry, and environmental solutions [72–74]. As it is impractical to cover all these applications here, our focus is on providing examples that illustrate how a new generation of chemical engineers is addressing mixing challenges in the manufacturing of advanced materials, including energy-storage materials, novel optical materials, and nanopesticides. Through mixing intensification, undesirable effects of the mixing state can be mitigated, enabling the effective scaling up of chemical reactions and ensuring high efficiency in industrial production. These examples underscore the importance of theoretical analysis in guiding engineering practices within the chemical industry.

3.1. Lithium battery precursor crystallization reactors and the intelligent manufacturing of high-end materials

The development of advanced material technologies for lithium batteries is a critical pathway to achieve China's "dual carbon" strategy. Precursors play a vital role in determining the performance of cathode materials. The preparation of ternary precursors involves a complex gas–liquid–solid three-phase system, where the crystallization process during co-precipitation reactions is rapid and governed by the micromixing of nickel, cobalt, and manganese metal salt ions with ammonium components. The inherent complexity of this process has limited the current understanding of the mechanisms controlling the precursor particle size, distribution, and morphology.

Scaling up gas–liquid–solid three-phase co-precipitation reaction crystallizers poses significant challenges. Researchers at the Institute of Process Engineering at the Chinese Academy of Sciences have addressed this issue by developing a multiphase CFD–micromixing–population balance equation (PBE) coupled model tailored to the rapid crystallization process. They further integrated the reaction and crystallization processes into a comprehensive CFD–PBE–PBE coupled model, specifically designed for gas–liquid–solid reaction crystallizers. Implemented using the OpenFOAM source code solver, this model represents a groundbreaking advancement in the field [75,76].

Additionally, a generalized high-precision finite-volume Kurganov–Tadmor (KT) method has been proposed for the discrete solution of the PBE in crystallization processes. This approach enables precise predictions of particle size and distribution [77]. These innovative numerical simulation methods and scaling-up tech-

Flow field obtained with the two-phase k - ϵ turbulent model

Improved precision for micromixing simulation by CFD-E-model

Fig. 5. Improved precision for micromixing simulation with the CFD-E-model compared with the engulfment model (E-model). k is kinetic energy, u_{tip} is velocity of impeller tip, and D is impeller diameter. vvm: air volume per culture volume per minute. Reproduced from Ref. [55] with permission.

niques for ternary precursor co-precipitation reaction crystallizers have led to the development of efficient new impellers. The resulting advancements facilitate the digital scaling of ternary precursor reaction crystallizers to capacities as large as 30 m³, achieving industrial precursors with narrow particle size distributions and high sphericity.

This technology has been successfully deployed in 2836 industrial reaction crystallization units across 103 precursor companies, accounting for more than 60% of ternary precursor manufacturers in China. As a result, the global capacity share of ternary precursors and cathode materials now exceeds 50%, driving the high-end, intelligent, and sustainable growth of China's lithium battery industry (Fig. 6) [77].

3.2. Micromixing intensification for the precise manufacturing of optical materials with a tunable refractive index

Optical materials with a tunable refractive index can be used to control and manipulate light, forming the foundation of optical devices such as encapsulants, lenses, and displays. Researchers have explored the incorporation of inorganic nanoparticles with

high refractive indices into organic resins to create nanocomposites with tunable optical properties. A major challenge in the scalable production of inorganic nanoparticles in liquid solutions is achieving homogeneous micromixing in reactors for fast and uniform crystallization. High-gravity technology, particularly the use of RPB reactors, has emerged as a promising process-intensification technique with significant industrial potential [78–81]. For example, He et al. [82] developed a process for synthesizing zirconia nanodispersions via high-gravity-assisted homogeneous precipitation in an internal circulation RPB reactor, followed by two-step modification. The mixing intensification achieved by the RPB reactor ensures homogeneous micromixing during the nucleation and growth of the zirconia particles, which facilitates the continuous and reproducible production of ultra-small zirconia nanoparticles with narrow size distributions (3–5 nm). The digital image in Fig. 7(a) shows highly dispersible zirconia nanoparticles on a sub-kilogram scale, with surface treatment [83]. These zirconia nanoparticles have been applied as coating materials in waterborne polyurethane to eliminate rainbow effects on polyester-based superficial hardening films [84]. In another study, precise control of the mixing process in the nanoparticle synthesis,

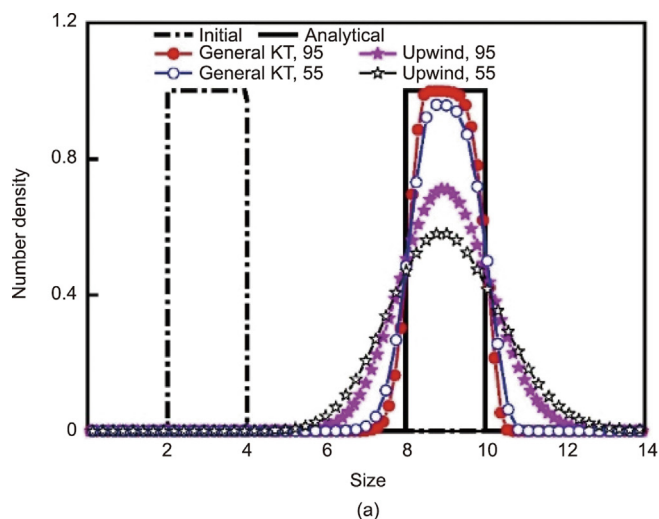


Fig. 6. (a) Comparison of numerical results obtained using different discrete schemes with two particle size grid numbers of 55 and 95; (b) industrial three-phase co-precipitation reaction crystallizers. (a) Reproduced from Ref. [77] with permission.

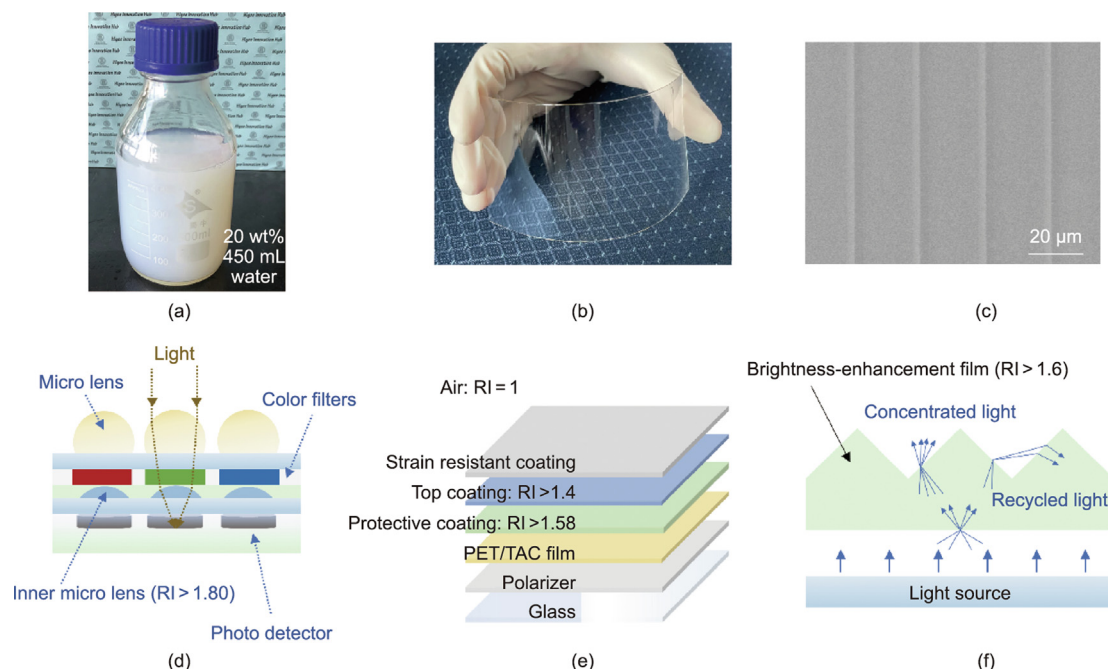


Fig. 7. (a) Digital picture of a nanoparticle dispersion; (b) digital picture of the organic–inorganic hybrid film; (c) scanning electron microscope image of UV-imprint patterns made of a hybrid resin; (d) a microlens array in a metal–oxide–semiconductor image sensor device; (e) schematic diagram of a liquid-crystal display structure with films with different refractive indices; (f) schematic diagram of a brightness-enhancement film. RI: refractive index; PET: polyethylene terephthalate; TAC: triacetyl cellulose. (a) Reproduced from Ref. [83] with permission; (b, c) reproduced from Ref. [85] with permission.

curing, and molding of nanocomposite films led to the development of a transparent photoresist made of titanium dioxide nanoparticle-embedded acrylic resin with a tunable refractive index for ultraviolet (UV)-imprint lithography (Figs. 7(b)–(f)) [85].

3.3. Scalable production of hollow silica nanoparticles for smart pesticide delivery toward sustainable agriculture

Achieving sustainable agricultural productivity remains one of the biggest challenges of the new millennium. Nanotechnology-based approaches have shown promising results for sustainable agricultural production, particularly in the development of innovative pesticides [86,87]. Nanosized particles, with their unique shapes and properties, are being explored for enhancing pesticide activity through nanocarrier formulations made from materials such as silica, lipids, polymers, copolymers, ceramics, metals, and carbon, among others [88]. Despite numerous studies on design strategies and synthetic methods for various nanopesticides and on the performance of such products, the widespread application of nanopesticides remains limited by the lack of low-cost, large-scale production capabilities that can ensure well-defined size and shape. Recently, significant progress has been made in the production of silica-based nanocarriers for pesticides, simplifying the synthesis operations and optimizing the reaction conditions for a greener, more sustainable approach [89]. Process-intensification technology, such as RPB reactors, can efficiently achieve uniform mixing at both macro and micro levels, allowing precise control over particle size at the nano and micron scales. This enables the efficient preparation of low-cost, high-quality hollow silica particles, which have shown great promise as novel, intelligent pesticide-delivery systems [90,91].

4. Perspectives

The integration of AI with multiphase flow measurement techniques is paving the way for transformative advancements in reactor design and process optimization. Leveraging advanced machine learning algorithms, AI has the potential to significantly enhance mixing

intensification—a critical factor in the performance of multiphase systems. The innovative bubSAM for bubble segmentation in chemical multiphase flow images exemplifies how foundational AI models can automate and refine the analysis of complex flow dynamics under real-time conditions. These capabilities highlight the adaptability of AI-driven approaches, which enable robust, scalable, and resource-efficient solutions for diverse operational scenarios.

AI-driven mixing intensification offers notable opportunities to optimize reaction kinetics and improve mass and heat transfer efficiencies, which are essential for achieving uniformity and stability in multiphase reactors. Future research should prioritize the integration of AI models with real-time feedback mechanisms to actively monitor and control mixing environments. For example, AI could predict optimal mixing parameters based on real-time data, thus reducing experimental costs and risks while improving precision in controlling chemical reactions. Additionally, the shift toward resource-efficient analytics underscores the potential to minimize reliance on large labeled datasets, reducing computational demands and making AI technologies more accessible for resource-constrained industrial settings. Coupled with AI's adaptability in process control, these advancements could lead to the development of next-generation reactors capable of precisely managing reaction parameters during complex multistep manufacturing processes.

Despite these promising developments, determining the optimal reactor type or technology for a specific industrial-scale process remains challenging. Practical applications require careful consideration of product quality and cost-effectiveness. In our view, the following avenues should be explored to address these challenges:

- (1) **Adopting advanced mixing technologies.** The application of innovative mixing methods, such as ultrasonic, electric-field, and magnetic-field mixing, should be investigated in order to manufacture advanced materials.
- (2) **Implementing multiscale simulation.** Multiscale simulation tools, spanning molecular to macroscopic levels, should be employed to gain deeper insights into physical and chem-

ical phenomena in the mixing processes of low-viscosity liquids and polymer systems, which will provide a solid theoretical foundation for molecular chemical engineering.

- (3) **Promoting interdisciplinary collaboration.** Cooperation among chemical engineering, materials science, physics, and related disciplines should be strengthened to drive the innovation and application of mixing technologies.
- (4) **Accelerating industrial translation.** The transformation of laboratory research into industrial applications should be focused on, particularly in the production of nanomaterials, optical materials, and new energy battery materials, to advance scientific progress and economic development.

By addressing these aspects of the field, we can move toward developing efficient reactors and advanced materials manufacturing processes that achieve precise control of reaction parameters and optimize multistep procedures.

Acknowledgment

This work was supported by the National Natural Science Foundation of China (22288102, 22035007, and 22122815).

Compliance with ethics guidelines

Chao Yang is an Editorial Board Member and Jian-Feng Chen is the Executive Editor-in-Chief for *Engineering*. Dan Wang is an Editorial Board Assistant of *Engineering*. They were not involved in the editorial review or the decision to publish this article. The other authors declare that they have no conflict of interest or financial conflicts to disclose.

References

- [1] Harnby N, Edwards MF, Nienow AW, editors. *Mixing in the process industries*. London: Butterworth-Heinemann Ltd.; 1985.
- [2] Mao ZS, Yang C. Micro-mixing in chemical reactors: a perspective. *Chin J Chem Eng* 2017;25(4):381–90.
- [3] Johnson BK, Prud'homme RK. Chemical processing and micromixing in confined impinging jets. *AIChE J* 2003;49(9):2264–82.
- [4] Rudolph G, Virtanen T, Ferrando M, Güell C, Lipnizki F, Kallioinen M. A review of *in situ* real-time monitoring techniques for membrane fouling in the biotechnology, biorefinery and food sectors. *J Membr Sci* 2019;588:117221.
- [5] Chen JF, Chen B, Li X, Rong S, Chen GT. Studies on micromixing in stirred tank reactors. I. High speed stroboscopic microscopic photography and its application. *Chem React Eng Techn* 1990;1:1–6. Chinese.
- [6] Huang D, Duan X, Feng X, Zhang W, Li Z, Mao ZS, et al. Image-based measurement of engulfment vortex to quantitatively assess micromixing efficiency in a gas–liquid stirred tank. *AIChE J* 2023;69(12):e18218.
- [7] Jasińska M. Test reactions to study efficiency of mixing. *Chem Process Eng* 2015;36(2):171–208.
- [8] Zhang YD, Zhang CL, Zhang LL, Sun BC, Chu GW, Chen JF. Chemical probe systems for assessing liquid–liquid mixing efficiencies of reactors. *Front Chem Sci Eng* 2023;17(10):1323–35.
- [9] Pečar D, Goršek A. Alkaline hydrolysis of an aromatic ester: kinetic studies using thermal power profiles. *Chem Eng Technol* 2011;34(12):2033–6.
- [10] Jasińska M, Bałdyga J, Cooke M, Kowalski A. Investigations of mass transfer with chemical reactions in two-phase liquid–liquid systems. *Chem Eng Res Des* 2013;91(11):2169–78.
- [11] Zhang YD, Wang ZX, Zhang LL, Sun BC, Chu GW, Chen JF. A consecutive-competitive reaction system for assessing homogeneous and heterogeneous liquid–liquid mixing efficiency. *AIChE J* 2022;68(11):e17824.
- [12] Li J, Tang Z, Zhang B, Xu C. Deep learning-based tomographic imaging of ECT for characterizing particle distribution in circulating fluidized bed. *AIChE J* 2023;69(5):e18055.
- [13] Wang W, Liu Q, Dong Y, Du J, Meng Q, Zhang L. ConvPred: a deep learning-based framework for predictions of potential organic reactions. *AIChE J* 2023;69(5):e18019.
- [14] Yao T, Liu J, Wan X, Li B, Rohani S, Gao Z, et al. Deep-learning based *in situ* image monitoring crystal polymorph and size distribution: modeling and validation. *AIChE J* 2024;70(2):e18279.
- [15] Xu H, Feng X, Pu Y, Wang X, Huang D, Zhang W, et al. BubSAM: bubble segmentation and shape reconstruction based on segment anything model of bubbly flow. *AIChE J* 2024;70(12):e18570.
- [16] Mao ZS, Yang C. Perspective to study on macro-mixing in chemical reactors. *CIESC J* 2015;66(8):2795–804.
- [17] Zhang T, Wang T, Wang J. Mathematical modeling of the residence time distribution in loop reactors. *Chem Eng Process* 2005;44(11):1221–7.
- [18] Nere NK, Patwardhan AW, Joshi JB. Liquid-phase mixing in stirred vessels: turbulent flow regime. *Ind Eng Chem Res* 2003;42(17):4146–56.
- [19] Ascanio G. Mixing time in stirred vessels: a review of experimental techniques. *Chin J Chem Eng* 2015;23(7):1065–76.
- [20] McManamey W. Circulation model for batch mixing in agitated, baffled vessels. *Chem Eng Res Des* 1980;58(4):271–6.
- [21] Joshi JB, Pandit AB, Sharmamm MM. Mechanically agitated gas–liquid reactors. *Chem Eng Sci* 1982;37(6):813–44.
- [22] Holmes D, Voncken R, Dekker J. Fluid flow in turbine-stirred, baffled tanks—I: circulation time. *Chem Eng Sci* 1964;19(3):201–8.
- [23] Fořt I, Valešová H, Kudrna V. Studies on mixing. XXVII. Liquid circulation in a system with axial mixer and radial baffles. *Collect Czech Chem Commun* 1971;36(1):164–85.
- [24] Brennan DJ, Lehrer IH. Impeller mixing in vessels experimental studies on the influence of some parameters and formulation of a general mixing time equation. *Chem Eng Res Des* 1976;54(A3):139–52.
- [25] Mann R, Mavros P. Analysis of unsteady tracer dispersion and mixing in a stirred vessel using interconnected network of ideal flow zones. In: Stephens HS, Goodes DH, editors. *Papers presented at the Fourth European Conference on Mixing*; 1982 Sep 15–17; Noordwijkerhout, the Netherlands. Cranfield: BHRA Fluid Engineering; 1982. p. 35–47.
- [26] Vrābel P, van der Lans RGJM, Luyben KCAM, Boon L, Nienow AW. Mixing in large-scale vessels stirred with multiple radial or radial and axial up-pumping impellers: modeling and measurements. *Chem Eng Sci* 2000;55(23):5881–96.
- [27] Fox RO. CFD models for analysis and design of chemical reactors. *Adv Chem Eng* 2006;31:231–305.
- [28] Li ZH, Xu HZ, Li YB, Sun BC, Chu GW. Determination of liquid residence time characteristics in spinning disk reactors via a computational approach. *Ind Eng Chem Res* 2023;62(38):15635–47.
- [29] Toson P, Doshi P, Jajcevic D. Explicit residence time distribution of a generalised cascade of continuous stirred tank reactors for a description of short recirculation time (bypassing). *Processes* 2019;7(9):615.
- [30] Klein JP, David R, Villermaux J. Interpretation of experimental liquid phase micromixing phenomena in a continuous stirred reactor with short residence times. *Ind Eng Chem Fundam* 1980;19(4):373–9.
- [31] Chen JF, Zheng C, Chen GA. Interaction of macro- and micromixing on particle size distribution in reactive precipitation. *Chem Eng Sci* 1996;51(10):1957–66.
- [32] Bourne JR, Yu S. Investigation of micromixing in stirred tank reactors using parallel reactions. *Ind Eng Chem Res* 1994;33(1):41–55.
- [33] Bałdyga J, Jasińska M, Trendowska J, Tadeusiak W, Cooke M, Kowalski A. Application of test reactions to study micromixing and mass transfer in chemical apparatus. *Tech Trans* 2012;109(5):11–20.
- [34] Fournier MC, Falk L, Villermaux J. A new parallel competing reaction system for assessing micromixing efficiency—experimental approach. *Chem Eng Sci* 1996;51(22):5053–64.
- [35] Huang D, Duan X, Feng X, Wang G, Zhang W, Chen J, et al. A novel highly sensitive test reaction for micromixing: acid–base neutralization and alkaline hydrolysis of ethyl oxalate. *AIChE J* 2025;71(2):e18615.
- [36] Bourne JR, Kozicki F, Rys P. Mixing and fast chemical reaction—I: test reactions to determine segregation. *Chem Eng Sci* 1981;36(10):1643–8.
- [37] Bourne JR, Kut OM, Lenzner J, Maire H. Kinetics of the diazo coupling between 1-naphthol and diazotized sulfanilic acid. *Ind Eng Chem Res* 1990;29(9):1761–5.
- [38] Zhang YD, Zhang LL, Wang ZX, Sun BC, Chu GW, Chen JF. Liquid–liquid heterogeneous mixing efficiency in a rotating packed bed reactor. *AIChE J* 2023;69(6):e18000.
- [39] Curl RL. Dispersed phase mixing: I. Theory and effects in simple reactors. *AIChE J* 1963;9(2):175–81.
- [40] Mehta RV, Tarbell JM. Four environment model of mixing and chemical reaction. Part I. Model development. *AIChE J* 1983;29(2):320–9.
- [41] David R, Villermaux J. Micromixing effects on complex reactions in a CSTR. *Chem Eng Sci* 1975;30(11):1309–13.
- [42] Fournier MC, Falk L, Villermaux J. A new parallel competing reaction system for assessing micromixing efficiency—determination of micromixing time by a simple mixing model. *Chem Eng Sci* 1996;51(23):5187–92.
- [43] Arian E, Pauer W. A comprehensive investigation of the incorporation model for micromixing time calculation. *Chem Eng Res Des* 2021;175:296–308.
- [44] Bałdyga J, Bourne JR. Simplification of micromixing calculations. I. Derivation and application of new model. *Chem Eng J* 1989;42(2):83–92.
- [45] Bałdyga J, Bourne JR. A fluid mechanical approach to turbulent mixing and chemical reaction. Part II. Micromixing in the light of turbulence theory. *Chem Eng Commun* 1984;28(4–6):243–58.
- [46] Li X, Chen G, Chen JF. Simplified framework for description of mixing with chemical reactions (I). Physical picture of micro- and macromixing. *Chin J Chem Eng* 1996;4(4):311–21.
- [47] Bakker RA, Van den Akker HE. A Lagrangian description of micromixing in a stirred tank reactor using 1D-micromixing models in a CFD flow field. *Chem Eng Sci* 1996;51(11):2643–8.
- [48] Li X. Theoretical and experimental study on micromixing [dissertation]. Hangzhou: Zhejiang University; 1992. Chinese.
- [49] Bakker RA, Van den Akker HE. A cylindrical stretching vortex model of micromixing in chemical reactors. In: *Proceedings of the 8th European Conference on Mixing*; 1994 Sep 18–20; Cambridge, England. Rugby: Institution of Chemical Engineers; 1994.

- [50] Fang JZ, Lee DJ. Micromixing efficiency in static mixer. *Chem Eng Sci* 2001;56(12):3797–802.
- [51] Yang HJ, Chu GW, Zhang JW, Shen ZG, Chen JF. Micromixing efficiency in a rotating packed bed: experiments and simulation. *Ind Eng Chem Res* 2005;44(20):7730–7.
- [52] Su Y, Chen G, Yuan Q. Ideal micromixing performance in packed microchannels. *Chem Eng Sci* 2011;66(13):2912–9.
- [53] Duan X, Feng X, Mao ZS, Yang C. Numerical simulation of reactive mixing process in a stirred reactor with the DQMOM-IEM model. *Chem Eng J* 2019;360:1177–87.
- [54] Duan X, Feng X, Yang C, Mao ZS. Numerical simulation of micro-mixing in stirred reactors using the engulfment model coupled with CFD. *Chem Eng Sci* 2016;140:179–88.
- [55] Duan X, Feng X, Peng C, Yang C, Mao ZS. Numerical simulation of micro-mixing in gas–liquid and solid–liquid stirred tanks with the coupled CFD-E-model. *Chin J Chem Eng* 2020;28(9):2235–47.
- [56] Chen L, Pan Z, Hu GH. Residence time distribution in screw extruders. *AIChE J* 1993;39(9):1455–64.
- [57] Hu GH, Kadri I, Picot C. On-line measurement of the residence time distribution in screw extruders. *Polym Eng Sci* 1999;39(5):930–9.
- [58] Zhang CL, Feng LF, Hoppe S, Hu GH. Residence time distribution: an old concept in chemical engineering and a new application in polymer processing. *AIChE J* 2009;55(1):279–83.
- [59] Zhang XM, Feng LF, Chen WX, Hu GH. Numerical simulation and experimental validation of mixing performance of kneading discs in a twin screw extruder. *Polym Eng Sci* 2009;49(9):1772–83.
- [60] Sun YJ, Hu GH, Lambla M, Kotlar HK. *In situ* compatibilization of polypropylene and poly(butylene terephthalate) polymer blends by one-step reactive extrusion. *Polymer* 1996;37(18):4119–27.
- [61] Hu GH, Cartier H, Plummer C. Reactive extrusion: toward nanoblends. *Macromolecules* 1999;32(14):4713–8.
- [62] Zhang CL, Feng LF, Hoppe S, Hu GH. Compatibilizer-tracer: a powerful concept for polymer-blending processes. *AIChE J* 2012;58(6):1921–8.
- [63] Ji WY, Feng LF, Zhang CL, Hoppe S, Hu GH, Dumas D. A concept of reactive compatibilizer-tracer for studying reactive polymer blending processes. *AIChE J* 2016;62(2):359–66.
- [64] Feng LF, Hu GH. Reaction kinetics at polymer–polymer interfaces under flow. *AIChE J* 2004;50(10):2604–12.
- [65] Ji WY, Li TT, Cheng SB, Feng LF, Gu XP, Zhang CL, et al. Two antagonistic effects of flow/mixing on reactive polymer blending. *AIChE J* 2022;68(11):e17835.
- [66] Ji WY, Feng LF, Zhang CL, Hoppe S, Hu GH. Development of a reactive compatibilizer-tracer for studying reactive polymer blends in a twin-screw extruder. *Ind Eng Chem Res* 2015;54(43):10698–706.
- [67] Li TT, Feng LF, Gu XP, Zhang CL, Wang P, Hu GH. Intensification of polymerization processes by reactive extrusion. *Ind Eng Chem Res* 2021;60(7):2791–806.
- [68] Devos C, Mukherjee S, Inguva P, Singh S, Wei Y, Mondal S, et al. Impinging jet mixers: a review of their mixing characteristics, performance considerations, and applications. *AIChE J* 2025;71(1):e18595.
- [69] Jilisen RTM, Bloemen PR, Speetjens MFM. Three-dimensional flow measurements in a static mixer. *AIChE J* 2013;59(5):1746–61.
- [70] Xu L, Jia Z, Guo M, Mao ZS, Fan Y, Zhang Q, et al. Enhancement of macromixing performance of a stirred tank with a novel V-shaped punched baffle. *Ind Eng Chem Res* 2023;62(8):3733–46.
- [71] Zhang LL, Wang JX, Liu ZP, Lu Y, Chu GW, Wang WC, et al. Efficient capture of carbon dioxide with novel mass-transfer intensification device using ionic liquids. *AIChE J* 2013;59(8):2957–65.
- [72] Salvachúa D, Saboe PO, Nelson RS, Singer C, McNamara I, del Cerro C, et al. Process intensification for the biological production of the ferul precursor butyric acid from biomass. *Cell Rep Phys Sci* 2021;2(10):100587.
- [73] Monjur MS, Hasan MMF. Computer-aided process intensification of natural gas to methanol process. *AIChE J* 2022;68(6):e17622.
- [74] Chen JF, Liu Y, Zhang Y. Control of product distribution of Fischer–Tropsch synthesis with a novel rotating packed-bed reactor: from diesel to light olefin. *Ind Eng Chem Res* 2012;51(25):8700–3.
- [75] Li Q, Cheng J, Yang C, Mao ZS. Simulation of a bubble column by computational fluid dynamics and population balance equation using the cell average method. *Chem Eng Technol* 2017;40(10):1792–801.
- [76] Li Q, Cheng J, Yang C, Mao ZS. CFD–PBE–PBE simulation of an airlift loop crystallizer. *Can J Chem Eng* 2018;96(6):1382–95.
- [77] Cheng J, Yang C, Jiang M, Li Q, Mao ZS. Simulation of antisolvent crystallization in impinging jets with coupled multiphase flow-micromixing-PBE. *Chem Eng Sci* 2017;171:500–12.
- [78] Koop J, Bera N, Quickert O, Schmitt M, Schlüter M, Held C, et al. Separation of volatile organic compounds from viscous liquids with RPB technology. *Ind Eng Chem Res* 2023;62(34):13637–45.
- [79] Huynh GH, Chen TL, Hsu CH, Chen YH, Chiang PC. Process integration of E-waste carbonization and high-gravity rotating packed bed for optimal gold recovery and the fine particles reduction. *Separ Purif Tech* 2020;241:116686.
- [80] Chang M, Wei Y, Liu D, Wang JX, Chen JF. A general strategy for instantaneous and continuous synthesis of ultrasmall metal–organic framework nanoparticles. *Angew Chem Int Ed* 2021;60(50):26390–6.
- [81] Wang F, Wang M, Liu Y, Pu Y, Wang JX, Wang D, et al. Intensified synthetic approach for GdYAG:Ce phosphors with ultrahigh color rendering toward healthy lighting. *AIChE J* 2024;70(1):e18253.
- [82] He X, Wang Z, Pu Y, Wang D, Tang R, Cui S, et al. High-gravity-assisted scalable synthesis of zirconia nanodispersion for light emitting diodes encapsulation with enhanced light extraction efficiency. *Chem Eng Sci* 2019;195:1–10.
- [83] He X, Wang Z, Wang D, Yang F, Tang R, Wang JX, et al. Sub-kilogram-scale synthesis of highly dispersible zirconia nanoparticles for hybrid optical resins. *Appl Surf Sci* 2019;491:505–16.
- [84] Liu Y, Wang X, Zhang B, Zhou Y, Pu Y, Wang JX, et al. Ultrastable waterborne nanocomposite coating of polyurethane and zirconia nanoparticles to avoid rainbow effect on polyester-based superficial hardening films. *Ind Eng Chem Res* 2024;63(1):244–51.
- [85] Liu Y, Wang D, Liu C, Hao Q, Li J, Wang JX, et al. A transparent photoresist made of titanium dioxide nanoparticle-embedded acrylic resin with a tunable refractive index for UV-imprint lithography. *Engineering* 2024;37:96–104.
- [86] Su Y, Zhou X, Meng H, Xia T, Liu H, Rolshausen P, et al. Cost-benefit analysis of nanofertilizers and nanopesticides emphasizes the need to improve the efficiency of nanoformulations for widescale adoption. *Nat Food* 2022;3(12):1020–30.
- [87] Wang D, Saleh NB, Byro A, Zepp R, Sahle-Demessie E, Luxton TP, et al. Nano-enabled pesticides for sustainable agriculture and global food security. *Nat Nanotechnol* 2022;17(4):347–60.
- [88] Chaud M, Souto EB, Zielinska A, Severino P, Batain F, Oliveira-Junior J, et al. Nanopesticides in agriculture: benefits and challenge in agricultural productivity, toxicological risks to human health and environment. *Toxics* 2021;9(6):131.
- [89] Chen JF, Wang K, Wang JX, Sun BC, Wang D, inventors; Beijing University of Chemical Technology, assignee. Method for rapidly preparing nano hollow silicon dioxide. China patent CN116282052. 2023 Jun 6. Chinese.
- [90] Wang K, Li JQ, He S, Lu J, Wang D, Wang JX, et al. Redox/near-infrared dual-responsive hollow mesoporous organosilica nanoparticles for pesticide smart delivery. *Langmuir* 2023;39(50):18466–75.
- [91] Wang K, Li JQ, Lu J, Wang D, He S, Wang JX, et al. Redox/pH dual-responsive fluorescent nanoparticles for intelligent pesticide release and visualization in gray mold disease synergistic control. *Langmuir* 2024;40(31):16511–20.